Keratin-dependent regulation of Aire and gene expression in skin tumor keratinocytes

Ryan P. Hobbs[1], **Daryle J. DePianto**[1,*], **Justin T. Jacob**[1,*], **Minerva C. Han**[1], **Byung-Min Chung**[1], **Adriana S. Batazzi**[1], **Brian G. Poll**[1], **Yajuan Guo**[1], **Jingnan Han**[1], **SuFey Ong**[2], **Wenxin Zheng**[1], **Janis M. Taube**[3,4], **Daniela Čiháková**[2,3], **Fengyi Wan**[1,5,7], and **Pierre A. Coulombe**[1,4,5,6,7]

[1]Department of Biochemistry and Molecular Biology, Bloomberg School of Public Health, Johns Hopkins University, Baltimore, MD 21205, USA

[2]Department of Molecular Microbiology and Immunology, Bloomberg School of Public Health, Johns Hopkins University, Baltimore, MD 21205, USA

[3]Department of Pathology, School of Medicine, Johns Hopkins University, Baltimore, MD 21205, USA

[4]Department of Dermatology, School of Medicine, Johns Hopkins University, Baltimore, MD 21205, USA

[5]Department of Oncology, School of Medicine, Johns Hopkins University, Baltimore, MD 21205, USA

[6]Department of Biological Chemistry, School of Medicine, Johns Hopkins University, Baltimore, MD 21205, USA

[7]The Sidney Kimmel Comprehensive Cancer Center, Johns Hopkins University, Baltimore MD 21205, USA

Abstract

Expression of the intermediate filament protein keratin 17 (K17) is robustly upregulated in inflammatory skin diseases and in many tumors originating in stratified and pseudostratified epithelia[1-3]. We report that Autoimmune regulator (Aire), a transcriptional regulator, is inducibly expressed in human and mouse tumor keratinocytes in a K17-dependent manner and required for a timely onset of *Gli2*-induced skin tumorigenesis in mice. Induction of *Aire* mRNA in keratinocytes depends upon a functional interaction between K17 and the heterogeneous nuclear

Address for correspondence: Pierre A. Coulombe, Ph.D., Dept. of Biochemistry and Molecular Biology, Johns Hopkins Bloomberg School of Public Health, 615 North Wolfe Street, Baltimore, MD 21205, USA. Tel: 410-955-3671. coulombe@jhsph.edu.
*contributed equally to this work.

ribonucleoprotein hnRNP K[4]. Further, K17 colocalizes with Aire protein in the nucleus of tumor-prone keratinocytes, and each are bound to a specific promoter region featuring a NF-κB consensus sequence in a relevant subset of K17- and Aire-dependent pro-inflammatory genes. These findings provide radically new insight into keratin intermediate filament and Aire function, along with a molecular basis for the K17-dependent amplification of inflammatory and immune responses in diseased epithelia.

Keywords

Keratin 17 (Krt17); Autoimmune regulator (Aire); hnRNP K; Skin; Inflammation; Cancer

Main text

High levels of *Krt17* expression have been correlated to aggressive behavior and poor prognosis for several types of human tumors[2]. Genetic loss of *Krt17*, but not the related *Krt14*, delays tumor onset in a *Gli2^tg* mouse model of basaloid skin tumorigenesis, correlating with striking changes in the amplitude and character of the inflammatory and immune responses[5]. Moreover, *Krt17* positively regulates several effectors of mitogenic signaling associated with oncogenic transformation, e.g., Akt/PKB[6], mTOR[7], and Rac1 GTPase[8], and is necessary to sustain normal Akt/PKB activation in the context of *Gli1*-mediated oncogenic transformation in Ewing Sarcoma[6]. Whether *Krt17* impacts additional types of tumors in a similar manner, and which mechanism(s) account for its influence, are unknown.

Targeted expression of the early genes from HPV type 16 (E1 to E7) to basal keratinocytes of epidermis causes tumors in adult mouse skin that resemble human skin squamous cell carcinoma[9]. Tumors arise with complete penetrance between postnatal day 60 (P60) and P120 in *HPV16^{tg/+}* ear skin (FVB/N strain) (Supplementary Fig. 1a), with no apparent gender discordance. While normally restricted to ectodermal appendages and glabrous skin[10], expression of K17 is robustly upregulated in the interfollicular epidermis between P20 and P40 in *HPV16^{tg/+}* mice (Supplementary Fig. 1b). Relative to *HPV16^{tg/+};Krt17^{+/+}*, *HPV16^{tg/+};Krt17^{-/-}* mice exhibit delayed hyperplasia and tumorigenesis in ear skin (Fig. 1a-b, Supplementary Fig. 1c). As had been observed in *Gli2^{tg/+};Krt17^{-/-}* mice[5], the delay correlates with profound reductions in key determinants of tumor growth including mitotic activity (Fig. 1c), blood vessel expansion (Supplementary Fig. 1d), inflammatory and immune response readouts (Supplementary Fig. 1e) including myeloperoxidase activity reflecting neutrophil infiltration (Fig. 1d), and dermal mast cell density (Fig. 1e). Transgene expression, p53 levels, and apoptosis are indistinguishable between genotypes in ear skin (Supplementary Fig. 1f-h). There is no indication of cell fragility in *HPV16^{tg/+}; Krt17^{-/-}* skin by electron microscopy (Supplementary Fig. 1i). Commercial qRT-PCR arrays identified many pro-inflammatory cytokines as being significantly depressed in tumor-prone ear tissue from *HPV16^{tg/+};Krt17^{-/-}* relative to controls (Supplementary Tables 1-5). Thus, the loss of *Krt17* delays tumorigenesis in mouse skin and significantly attenuates the expression of several key pro-inflammatory signaling molecules in two oncogenic paradigms (*Gli2^{tg}* and

HPV16[tg]) involving strains that are differentially sensitive to skin carcinogenesis (C57Bl/6 and FVB/N)[11].

To explore how pro-inflammatory gene expression may be regulated by K17, we devised a custom, 96-well plate based, real-time PCR (qRT-PCR) assay to quantitate mRNA levels for inflammation- and disease-relevant genes (Supplementary Table 6) in A431 cells (derived from a human epidermoid carcinoma and K17-expressing[1]). Twenty-two genes were consistently upregulated (>2-fold) in A431 cells following treatment with TPA (Supplemental Fig. 2a), which elicits a robust inflammatory response in keratinocytes[12]. Of those, nineteen are similarly upregulated in P40 HPV16[tg/+] ear tissue (Fig. 2a). Compared to non-silencing shRNA control, A431 cells with stable KRT17 knockdown[13] exhibit a significantly attenuated response to TPA (Supplemental Fig. 2a). Re-introduction of K17, but not the highly homologous K42[14], largely restored TPA-dependent cytokine upregulation in A431 cells (Supplementary Fig. 2b). Therefore, the expression of multiple pro-inflammatory cytokines also depends on KRT17 in human skin tumor keratinocytes.

Several observations converged on Aire (Autoimmune regulator), a transcriptional regulator with a well-known role in the medullary thymus towards the establishment of tolerance[15-17], as a component of the K17-mediated regulation of gene expression in skin keratinocytes. First, mutation in AIRE causes autoimmune polyendocrinopathy-candidiasis-ectodermal dystrophy (APECED)[18], which often presents with ectodermal anomalies in tissues that express Krt17[10] (e.g., alopecia, nail dystrophy, vitiligo, enamel hypoplasia). Second, several of the pro-inflammatory genes determined to be Krt17-dependent in tumor-prone keratinocytes (Supplemental Fig. 2a) are Aire-dependent in thymic epithelial cells (e.g., Ccl19, Ccl22, Cxcl5, Ccr7, Il6, Cd40)[19-21]. Third, qRT-PCR and/or RNA in situ hybridization show that Aire mRNA expression is induced and Krt17-dependent in several settings including TPA-treated human A431 cells (Fig. 2b), ear tissue from P40 HPV16[tg/+] (Fig. 2b,d) and P70 Gli2[tg/+] mice (Fig. 2b), and TPA-treated ear skin of C57bl/6 and FVB/N wild-type mice (Fig. 2c, Supplemental Fig. 2c). Sense strand controls yielded negative findings (Supplemental Fig. 2d-e). Aire expression is low in untreated or wild-type skin (Fig. 2c-d)[22]. The observed levels of induced Aire mRNA in treated or diseased skin remain below constitutive levels in the thymus (Supplemental Fig. 2c). Fourth, there is a report of a physical interaction between Aire and K17 proteins[23], which we confirmed (Supplementary Fig. 2f). Finally, we crossed Aire^{-/-} with Gli2[tg/+] mice (both available in the C57Bl/6 strain) to assess the impact of Aire loss on skin tumorigenesis (Fig. 2e). The average age of tumor onset was 79 ± 3.7 (s.e.m.) days in male Gli2[tg/+];Aire^{-/-} mice, compared to 65 ± 3.9 days in Gli2[tg/+] mice (p<0.001). A similar delay was previously reported for Gli2[tg/+];Krt17^{-/-} mice[5] (Fig. 2f).

Importantly, Aire expression is not Krt17-dependent in the medullary thymus (Supplemental Fig. 3a-b), which expresses Krt17[10]. Further, loss of Krt17 does not induce a break in central tolerance leading to systemic autoimmunity, unlike the case for Aire loss[24] (Supplemental Fig. 3c-e). Our findings thus reveal a novel and significant role for extra-thymic Aire expression in keratinocytes, particularly during skin tumorigenesis, where its expression depends upon Krt17.

We next investigated how *Aire* mRNA levels depend upon K17. The ribonucleoprotein hnRNP K, a versatile regulator of gene expression with a known role during tumorigenesis[25], physically and functionally interacts with K17 to impact the expression of the Cxcr3 ligands *Cxcl9*, *Cxcl10*, and *Cxcl11* along with several other cytokines in tumor skin keratinocytes[4]. We report here that the *Aire* mRNA is also bound to hnRNP K, in a TPA- as well as K17-dependent manner, in human A431 and in mouse *Gli2^tg* keratinocytes (Fig. 2g-h). The TPA-dependent induction of *Aire* mRNA is markedly attenuated following siRNA-mediated hnRNP K knockdown in A431 keratinocytes (Fig. 2i). Overexpression of hnRNP K suffices to induce *Aire* levels in A431 cells, again in a *Krt17*-dependent manner (Fig. 2j). Thus, *Aire* mRNA transcripts are regulated in a K17-and hnRNP K-dependent manner in skin tumor keratinocytes.

We next assessed whether K17 also regulates Aire at the protein level. Consistent with previous reports[26, 27], transfected Aire fusion proteins frequently localize to round and smooth surfaced punctae in the nucleus and cytoplasm of human A431 cells (Fig. 3a) and mouse keratinocytes (data not shown) in the absence of stimulus. These Aire-positive punctae are distinct from lysosomes or stress granules, but occur immediately adjacent nuclear PML bodies (Supplemental Fig. 4a), which are associated with the storage of proteins poised for transcriptional activation[28]. Further, heat shock protein 70 (HSP70), previously identified to associate with Aire[29] and keratin[30], colocalizes with the Aire-positive nuclear punctae and does so in a *Krt17*-dependent manner (Supplemental Fig. 4b). Strikingly, within 1 hr of TPA treatment, the nuclear localization pattern of Aire shifts from punctate to diffuse (Fig. 3a). This shift is markedly hindered in sh*Krt17*-expressing A431 lines (Fig. 3a), though the punctae eventually diffuse later (6-12 hr; data not shown). Collectively, these findings indicate that K17 physically interacts with Aire and impacts its sub-nuclear distribution in response to TPA (a process that may require HSP70 association), towards the induction of target gene expression.

We next asked whether K17 might also localize to the nucleus (along with Aire) in keratinocytes. In the presence of leptomycin B (LMB), which inhibits exportin 1-dependent nuclear export (thereby trapping low abundancy or rapidly-shuttling proteins[31]), K17 occurs in the form of intra-nuclear punctae in human A431 keratinocytes (Fig. 3b), where it readily colocalizes with transfected Aire protein (Fig. 3c), and in HeLa cells (Supplemental Fig. 4c-d). Intra-nuclear K17 also occurs in LMB-treated mouse epidermal keratinocytes in primary culture, where it colocalizes with type II partner K5 (Supplemental Fig. 4e). No evidence of nuclear (or any form of) K17 could be detected in LMB-treated *Krt17^-/-* mouse keratinocytes (Supplemental Fig. 4f), establishing the specificity of our reagents. Occurrence of K17 and Aire in the nucleus is further supported by western blot analyses performed on subcellular fractions from non-LMB treated cells, including one enriched for nucleoplasmic proteins (e.g., Histone H3) and devoid of nuclear envelope markers (Supplemental Fig. 4g). By contrast K14 or K18, which also occur in A431 keratinocytes, do not yield the same fractionation pattern and have not been observed in the nucleus under these assay conditions (Supplementary Fig. 4h). Furthermore, nuclear K17 can be readily observed in tumor keratinocytes in tissue sections prepared from biopsies of skin basal cell carcinomas from patients (Fig. 3d). Bioinformatic analyses revealed a putative nuclear localization sequence

(NLS) within the K17 sequence[32] (Fig. 3e), a dilysine motif in the tail domain, which is conserved across species for K17, but not present in other type I intermediate filament proteins. Relative to wild-type K17, transient transfection of GFP-K17 (either human or mouse sequence) harboring a single point mutation within the putative NLS (p.Lys399Ala) into *Krt17*^{-/-} A431 keratinocytes (see methods) is sufficient to attenuate the ability of K17 to: i) localize to the nucleus (Fig. 3f); ii) co-localize with nuclear mCherry-Aire punctae (Fig. 3g), and iii) foster a full cytokine expression response following TPA (Fig. 3h). These findings establish that K17 can occur in the nucleus, and suggest that the nuclear form of K17 may play a role in the rapid dispersion of the normally quiescent Aire-containing nuclear punctae following a relevant stimulus.

Though not believed to directly bind DNA[33], Aire binds a plethora of transcriptional proteins to activate target gene expression[20, 31]. Chromatin immunoprecipitation (ChIP) assays were conducted to assess whether Aire protein, along with K17, each occur at the promoter of relevant inflammatory and immune response genes in tumor-prone keratinocytes (see Supplementary Table 7). Using RFP-trap beads in mCherry-Aire transfected A431 cells (with mCherry vector as control), ChIP analysis revealed enrichment for specific segments within the proximal 5′ upstream region for *MMP9, CCL19, CXCL10* and *CXCL11*, but not control, genes (Fig. 4a-b). Endogenous K17 can be readily immunoprecipitated from nuclear fractions prepared from A431 cells, whether TPA-treated or not (Supplemental Fig. 5a). Following TPA, specifically, the same or adjacent segments within the *MMP9, CCL19, CXCL10*, and *CXCL11* gene promoters are enriched in K17 IPs (Fig. 4c-d). No enrichment was observed after DMSO treatment or with pre-immune serum IP. We verified that PCR-amplified promoter fragments migrate at the expected size upon gel electrophoresis (Supplementary Fig. 5b). These ChIP findings indicate K17 and Aire each associate with the same promoter regions of select *Krt17*-dependent target genes.

Analysis of the promoter segments enriched in ChIP samples for mCherry-Aire and K17 revealed the presence, in all cases, of consensus binding sites for NF-κB (5′-GGGRNNYYCC-3′)[34] (Supplemental Fig. 5c-d). NF-κB plays a keratinocyte-autonomous role in skin inflammatory conditions[35], and thus represents an ideal candidate to mediate the recruitment of K17 to relevant gene promoters. Electrophoretic mobility shift assays confirm that a protein complex associates with a NF-κB consensus oligonucleotide probe in a TPA-dependent manner in nuclear extracts prepared from A431 keratinocytes (Fig. 4e-f). Adding antisera against either K17 or the NF-κB subunit p65 yields a supershift in the mobility of the NF-κB probe, only in the presence of TPA (Fig. 4e). The use of pre-immune sera or anti-IgG control antibodies (Fig. 4e), excess unlabeled oligonucleotide as competitor (Fig. 4f), or non-TPA induced Oct1 oligonucleotide (Supplemental Fig. 5e) confirms specificity. Lastly, reciprocal co-IPs indicate that endogenous K17 and p65 interact in A431 keratinocytes (Supplemental Fig. 5f). p65/NF-κB thus may act as a molecular bridge between K17 and Aire at promoter sequences for the specific set of genes they co-regulate in tumor-prone skin keratinocytes.

In concluding, the findings reported here establish a novel role for K17 in regulating gene expression at the transcriptional level in skin keratinocytes, which involves a nuclear-localized form of this keratin protein (Fig. 4g). They provide a mechanistic basis for a

positive feedback loop whereby K17 upregulation, an early event when inflammation sets in, would promote the maintenance of a specific type of pro-inflammatory and immune response in skin. Lastly, they also establish the involvement of Aire in promoting gene expression in keratinocytes and skin undergoing acute inflammation or tumorigenesis, a newly defined role that requires a physical and functional partnership with K17.

Online Methods

Mouse Models

All protocols involving mice were approved by the Johns Hopkins Institutional Care & Use Committee. C57BL/6 *Krt17*^{-/-} mice[36] were bred to the *HPV16*[tg/+] transgenic mice (FVB/N strain, obtained from the National Cancer Institute) to create *HPV16*[tg/+];*Krt17*^{-/-} mice. The resulting *HPV16*[tg/+];*Krt17*^{+/-} mice were back-crossed with wildtype FVB/N mice for at least 6 generations. To generate *Gli2*[tg/+];*Aire*^{-/-} mice, C57Bl/6 *Aire*^{+/-} mice were obtained from Jackson Laboratories (stock #006360) and bred with C57Bl/6 *Gli2*[tg/+] mice; *Gli2*[tg/+];*Aire*^{+/-} mice were crossed with *Aire*^{+/-} littermates to generate the progeny of interest. All mice with tumor transgenes were housed individually or with littermate controls upon weaning, and fed rodent chow and water *ad libitum*. Both male and female mice were used in this study. The sample size of mice required for this study was empirically determined from previous experience[5]. Mice deemed sickly by veterinary staff were not utilized. Investigator blinding and randomization were not conducted. Genotyping protocols have been previously described for the *Gli2*[tg][5], *Krt17*[5], *HPV16*[tg] (National Cancer Institute Mouse Repository, strain code #01XT3), and *Aire* alleles (Jackson Laboratories, stock #006360).

Cell lines

Mouse epidermal keratinocytes were isolated for primary culture or immortalized as described[37]. Parental A431 and HeLa cell lines (ATCC) were confirmed to be mycoplasma free (data not shown). Generation of A431 cells stably expressing sh*Krt17* has been reported[13]. Generation of A431 cells null for K17 was conducted by CRISPR-Cas9-mediated genome engineering[38]. Specifically, a target sequence in the first exon of human KRT17 (5′-GGCTCCTCCGGCCTGGGGGGCGG-3′ (PAM motif underlined)) was chosen and a 20-nucleotide guide sequence (5′-GGCTCCTCCGGCCTGGGGGG-3′) was cloned into the BbsI site of pX458 (pSpCas9(BB)-2A-GFP; obtained from Addgene (plasmid #48138)) according to the cloning protocol[38]. For sequencing purpose, targeted K17 regions in the knockout cell line were PCR amplified and cloned into a pJET1.2/blunt cloning vector using the CloneJET™ PCR Cloning Kit (Life Technologies, #K1231). Sequencing results showed a frameshift and premature stop codon formation at both alleles of K17 (data not shown).

Antibodies, reagents, and plasmid constructs

The primary antibodies utilized in this study included: rabbit polyclonal against Krt17[10], phospho-histone H3 (Cell Signaling #9701), Histone H3 (Cell Signaling #9715), mCherry (BioVision #5993), p65 (Santa Cruz #SC-372X), and Nesprin-3 (GeneTex #GTX87974); goat polyclonal against eIF3η (Santa Cruz #SC-13677) and p53 (Santa Cruz #SC-315);

chicken polyclonal against Krt14 (Covance #AF64) and Krt5 (Covance #AF138); rat polyclonal against CD11b (eBiosciences #11-0112-81), CD207 (eBiosciences #14-2075-82), CD4 (BD Biosciences #550280), and CD45 (eBiosciences #45-0451-80); hamster polyclonal against CD11c (eBiosciences #17-0114-81); and mouse monoclonal against PECAM-1 (Chemicon #CBL1337), Hsp70 (StressGen #ADI-SPA-812), LAMP-1 (DSHB, University of Iowa #H4A3), Actin (Sigma #A5441), GAPDH (Santa Cruz #SC-365062), IκBα (Cell Signaling #4814), E7 (Invitrogen #28-0006), hnRNP K (Santa Cruz #SC-32307) and PML (Santa Cruz #SC-966). Secondary antibodies utilized include Alexa 488, Alexa 594, and Alexa 647 (Invitrogen) for indirect immunofluorescence, and horseradish peroxidase conjugated goat-anti-mouse, goat-anti-rabbit, and rabbit-anti- goat (Sigma) for chemiluminescence Western blotting. DNA was immunostained using Hoescht (Sigma). All commercial antibodies were used according to manufacturer's recommendation. TUNEL (Roche #11767291910) staining for apoptotic cells was done according to the manufacturer's instruction. TPA (Sigma #P1585) was dissolved in DMSO (for cell treatments) or acetone (for ear tissue topical treatment) and used at 200 nM or 25 ng/mL working concentration, respectively. Leptomycin B (LMB; Sigma #L2913) was dissolved in 70% methanol and used at 40.7 nM working concentration.

A full-length human Aire cDNA clone (a gift from P. Peterson) was moved into a mCherry-C1 vector (Clontech) using HindIII and SacII restriction enzymes, generating mCherry-Aire. mCherry and mCherry-Aire plasmids were transiently transfected into A431 cells using FuGene HD (Promega #E2311)) at a 1:3 (DNA amount:FuGene volume) ratio according to manufacturer's instruction. siRNA oligonucleotides targeting hnRNP K and their transfection protocol have been previously described[4]. Overexpression of hnRNP K from plasmid has been described[4]. The GFP-K17 K399A mutant was generated from pEGFP-C3-K17 wild-type plasmid using the Phusion mutagenesis kit (Life Technologies #F-541).

Tissue harvesting and morphological analyses

Histological assays for all ear tissue sections[5] and electron microscopy[39] were conducted as described. Epidermal thickness measurements, image quantitation, and myeloperoxidase assay were done as described[5, 39]. Basal cell aspect ratio was determined by dividing length and width of individual basal cells using the ImageJ software. Immunohistochemistry and immunofluorescence images were acquired using a Zeiss fluorescence microscope with Apotome attachment. Confocal immunofluorescence images were acquired using a Zeiss LSM 710. Images from like experiments were equally brightened, contrasted, and cropped using ImageJ software for optimal presentation.

For analysis of autoinflammation, all tissues were obtained from male mice between 4-10 months of age (n=4-5, per genotype). Tissues were embedded longitudinally in paraffin, and 5-μm sections were cut and stained with H&E or Masson's Trichrome Blue (Histoserv) prior to microscopic evaluation and grading. Grading was performed by two independent blinded investigators and averaged.

De-identified samples from paraffin embedded blocks of diagnostic biopsies for human basal cell carcinomas were used for immunofluorescence analysis also under Hopkins IRB

protocol approval (NA_00072381). Tissue sections were immunostained for K17 and Hoechst and images were acquired with Apotome attachment as stated above.

Flow cytometry

Mouse ears were harvested, washed with PBS, split into halves, and placed in 0.4 mg/mL Liberase (Roche #05-401-054-001) diluted in serum-free RPMI 1640 containing 5% penicillin/streptomycin for 1.5 hr at 37°C. Liberase was inactivated by adding complete RPMI 1640 containing 5% FCS and tissues were manually homogenized by syringe prior to passage through a 70 μm-pore filter and centrifugation at $200 \times g$ for 8 min. Cells were resuspended in PBS and centrifuged in a 30%-70% Percoll gradient (GE Healthcare #17-0891-01). Mononuclear cells at the gradient interface were collected, washed, resuspended in PBS, incubated with 5 μg/mL FcR blocker (anti-CD16/CD32, eBioscience), washed with PBS, and resuspended in staining buffer (1% fetal calf serum in PBS) prior to labeling with respective antibodies for 30 min on ice. After washing twice with staining buffer, cells were collected by FACS Calibur (BD Biosciences) and analyzed using FlowJo (Tree Star).

RNA in situ hybridization

Aire sense and antisense probes were generated by PCR subcloning a 418 bp fragment from a mouse Aire cDNA plasmid[40] (provided by P. Peterson, Tartu University, Estonia) into the pCR II-TOPO vector (forward primer: 5′-AAGAAGCCAGATGGCAACTT-3′; reverse primer: 5′-ACACGGCACACTCATCCTCG-3′. In vitro transcription using T7 (Ambion #2082) and Sp6 (Ambion #2071) polymerases yielded sense and antisense probes, which were labeled with DIG and purified using illustra microspin G-50 columns (GE Healthcare #27-5330-01). 5 μL of probe was used per slide. For TPA treatment, one mouse ear was treated four times, 48-hrs apart from each other, with 25 ng/mL TPA, with the other ear of the same mouse treated with acetone as a control. ISH protocol was conducted as previously reported. The time of alkaline phosphatase reaction was the same for all samples. Four sets of biological replicates were utilized, with one representative being depicted.

Protein extraction, subcellular fractionation, and co-immunoprecipitation

Protein lysates for Western blotting were prepared in urea sample buffer (8 M deionized urea, 0.5% SDS, 30 mM Tris pH6.8, 5% glycerol, 5% β-ME) after homogenization (ear tissue) or PBS washing (cultured cells). All samples were sheared using progressive gauged needles (22 ½, 25 ½, 26 ½) and subjected to a Bradford assay and processed for Western blotting analysis as previously described[5]. Subcellular fractionation was conducted based on correspondence with R. Foisner (Max F. Perutz Laboratories). After $3\times$ PBS rinsing on ice, cells were scraped into a hypotonic lysis buffer (10 mM Tris pH7.5, 1 mM $MgCl_2$, 10 mM KCl plus protease inhibitors), incubated on ice for 10 minutes, and sheared with 20½ gauge needle to release nuclei. After spinning down at 3000 rpm for 5 minutes, supernatant was removed (soluble fraction) and pelleted nuclei were resuspended in nuclear envelope extraction buffer (20 mM HEPES pH7.9, 420 mM NaCl, 1% Triton-X 100, 1.5 mM $MgCl_2$, 0.2 mM EDTA plus protease inhibitors), and twice incubated on ice for 10 min followed by 1 min vortex prior to spinning at 13,000 rpm for 10 minutes. The supernatant containing

nuclear envelope (NE) was retained. The pellet containing histones (Chr) was resuspended in urea sample buffer. Sol, NE, and Chr samples were electrophoresed on 10% SDS-PAGE and subjected to Western blot analysis using relevant markers.

Immunoprecipitation for Krt17, p65, and hnRNP K was conducted as previously described[4, 34]. mCherry and mCherry-Aire were immunoprecipitated using 10 µL RFP-trap beads (Chromotek) per sample incubated for 1 hr at 4°C with rotation. HPV16 E7 protein was immunoprecipitated from P2 mouse skin subjected to the Dynabeads co-immunoprecipitation kit (Invitrogen) containing protease inhibitors. Protein content was determined by Bradford assay, and 1.5 mg of HPV16 E7 antibody or rabbit IgG was coupled to Dynabeads which, after clearing, were incubated with extracted proteins for 1 hr at 4°C. After washing and elution, IP samples were then electrophoresed by SDS-PAGE and subjected to Western blot analysis. RNA-immunoprecipitation was conducted as previously described[4].

Quantitative real-time polymerase chain reaction (qRT-PCR)

Commercial qRT-PCR plates (SABiosciences; #PAMM-011A, #PAMM-025, #PAMM-073, #PAMM-014A, and #PAMM-052) were performed on ear tissue samples from P40 *HPV16*$^{tg/+}$ and *HPV16*$^{tg/+}$;*K17*$^{-/-}$ mice. Custom qRT-PCR assays were performed on ear tissue samples from P80 *Gli2*$^{tg/+}$ and *Gli2*$^{tg/+}$;*Krt17*$^{-/-}$, P40 *HPV16*$^{tg/+}$ and *HPV16*$^{tg/+}$;*K17*$^{-/-}$ mice, and A431 cells stably expressing control or sh*Krt17* plasmids. Total RNA from ear tissue was isolated using Trizol (Invitrogen), followed by DNAseI treatment (Qiagen) and cleanup on RNeasy Mini column (Qiagen). RNA from A431 cells was isolated using the RNEasy kit (Qiagen). All RNA concentration and purity was assessed by spectrophotometry. 1 µg of RNA was reverse-transcribed with the RT^2 First strand Kit (Qiagen) or iScript (BioRad). qRT-PCR was performed on the first strand cDNA using the RT^2 Profiler PCR Array (Qiagen) or SSO-Advanced SYBR green (BioRad) as described by the manufacturer. PCR parameters for custom qRT-PCR screen = 95°C for 5 minutes, followed by 40 cycles of 95°C for 10 sec + 55°C for 30 sec. No template controls, no reverse-transcriptase controls, standard curves, and a melt curve were included with every PCR plate. Data analysis for commercial qRT-PCR arrays was performed using the template provided online by SABiosciences. Normalized expression values for custom qRT-PCR data were determined using Microsoft Excel by first averaging the relative expression for each target gene ($2^{-(C_q \text{target gene}-C_q \text{reference gene})}$) across all biological replicates and then dividing the relative expression value of the experimental condition by the control condition ($2^{-(\triangle C_q \text{Experimental}- \triangle C_q \text{Control})}$). Error bars are derived from standard error of $\triangle C_q$ values ($C_q$target gene-$C_q$reference gene) across all biological replicates. *ACTB*, *GAPDH*, and *RPS18* were all used as reference genes. Normalized expression values for each target gene in all qRT-PCR experiments are derived from at least 3 biological replicates. A list of all custom qRT-PCR primers utilized is provided in Supplementary Tables 2 and 3.

Chromatin immunoprecipitation

Cells were treated with DMSO or TPA for 3 h at 37°C, 5% CO_2 prior to execution of the ChIP protocol as described[41]. 1 µL of anti-Krt17 antibody or pre-immune sera was incubated per mg of total protein for all K17 ChIP assays. 10 µL of RFP-trap beads were

used per IP condition for all mCherry-Aire ChIP assays. Antibody incubations occurred overnight at 4°C. The eluates were precipitated and resuspendend in 60 μL of sterile H_2O with 1 μL used per PCR reaction (40 cycles) with SSO Advanced SYBR green mix (Bio-Rad) and primers as outlined in Supplemental Information. PCR products were separated by 1.5% agarose electrophoresis.

Electorphoretic mobility shift assays (EMSAs)

EMSAs were conducted using the EMSA kit (Promega) as previously described[42] with modifications. A431 keratinocytes were serum-starved for 24-hrs followed by 1-hr treatment with TPA (200 nM) prior to isolation of nuclear extracts. For supershift analyses, nuclear extracts were incubated with 1 μL of either rabbit-IgG (Source), rabbit anti-p65 (Cell Signaling), pre-immune sera[10], or anti-K17[10] antibodies for 15 minutes at room temperature prior to incubation with ^{32}P-labeled NF-κB oligonucleotide. For competition binding analyses, 50-fold excess non-labeled NF-κB or Oct1 (as a control) oligonucleotide was incubated for 15 minutes at room temperature with nuclear extract prior to incubation with ^{32}P-labeled NF-κB oligonucleotide. Oligonucleotide labeling and gel shift assays were conducted following manufacturer's protocol (Promega, Gel Shift Assay System). Samples were resolved on a 6% DNA retardation gel (Invitrogen) in $0.5 \times$ TBE buffer. Autoradiography was carried out on dried gels using phosphor-screens and phosphorimager.

Description of statistical methods

All error bars represent the standard deviation across biological replicates divided by the square root of the sample size (s.e.m.). Where technical replicates were conducted, these values were averaged to yield a single value per biological replicate. All p values were obtained by simple t-test with two-sided distribution and equal variance (Microsoft Excel), except as stated in Supplementary Figure 3.

Supplementary Material

Refer to Web version on PubMed Central for supplementary material.

Acknowledgments

References

1. Moll R, Franke WW, Schiller DL, Geiger B, Krepler R. The catalog of human cytokeratins: patterns of expression in normal epithelia, tumors and cultured cells. Cell. 1982; 31:11–24. [PubMed: 6186379]

2. Karantza V. Keratins in health and cancer: more than mere epithelial cell markers. Oncogene. 2011; 30:127–138. [PubMed: 20890307]

3. Jin L, Wang G. Keratin 17: a critical player in the pathogenesis of psoriasis. Med Res Rev. 2014; 34:438–454. [PubMed: 23722817]

4. Chung BM, et al. Regulation of C-X-C chemokine gene expression by keratin 17 and hnRNP K in skin tumor keratinocytes. J Cell Biol. 2015; 208:613–627. [PubMed: 25713416]

5. Depianto D, Kerns ML, Dlugosz AA, Coulombe PA. Keratin 17 promotes epithelial proliferation and tumor growth by polarizing the immune response in skin. Nat Genet. 2010; 42:910–914. [PubMed: 20871598]

6. Sankar S, et al. A novel role for keratin 17 in coordinating oncogenic transformation and cellular adhesion in Ewing sarcoma. Mol Cell Biol. 2013; 33:4448–4460. [PubMed: 24043308]

7. Kim S, Wong P, Coulombe PA. A keratin cytoskeletal protein regulates protein synthesis and epithelial cell growth. Nature. 2006; 441:362–365. [PubMed: 16710422]

8. Chen R, et al. Rac1 regulates skin tumors by regulation of keratin 17 through recruitment and interaction with CD11b+Gr1+ cells. Oncotarget. 2014; 5:4406–4417. [PubMed: 24962779]

9. Arbeit JM, Munger K, Howley PM, Hanahan D. Progressive squamous epithelial neoplasia in K14-human papillomavirus type 16 transgenic mice. J Virol. 1994; 68:4358–4368. [PubMed: 7515971]

10. McGowan KM, Coulombe PA. Onset of keratin 17 expression coincides with the definition of major epithelial lineages during skin development. J Cell Biol. 1998; 143:469–486. [PubMed: 9786956]

11. Woodworth CD, et al. Strain-dependent differences in malignant conversion of mouse skin tumors is an inherent property of the epidermal keratinocyte. Carcinogenesis. 2004; 25:1771–1778. [PubMed: 15105299]

12. Mueller MM. Inflammation in epithelial skin tumours: old stories and new ideas. Eur J Cancer. 2006; 42:735–744. [PubMed: 16527478]

13. Lee CH, Kim MS, Chung BM, Leahy DJ, Coulombe PA. Structural basis for heteromeric assembly and perinuclear organization of keratin filaments. Nat Struct Mol Biol. 2012; 19:707–715. [PubMed: 22705788]

14. Tong X, Coulombe PA. A novel mouse type I intermediate filament gene, keratin 17n (K17n), exhibits preferred expression in nail tissue. J Invest Dermatol. 2004; 122:965–970. [PubMed: 15102087]

15. Laan M, Peterson P. The Many Faces of Aire in Central Tolerance. Front Immunol. 2013; 4:326. [PubMed: 24130560]

16. Mathis D, Benoist C. A decade of AIRE. Nat Rev Immunol. 2007; 7:645–650. [PubMed: 17641664]

17. Metzger TC, Anderson MS. Control of central and peripheral tolerance by Aire. Immunol Rev. 2011; 241:89–103. [PubMed: 21488892]

18. Kisand K, Peterson P. Autoimmune polyendocrinopathy candidiasis ectodermal dystrophy: known and novel aspects of the syndrome. Ann N Y Acad Sci. 2011; 1246:77–91. [PubMed: 22236432]

19. Sillanpaa N, et al. Autoimmune regulator induced changes in the gene expression profile of human monocyte-dendritic cell-lineage. Mol Immunol. 2004; 41:1185–1198. [PubMed: 15482854]

20. Giraud M, et al. Aire unleashes stalled RNA polymerase to induce ectopic gene expression in thymic epithelial cells. Proc Natl Acad Sci U S A. 2012; 109:535–540. [PubMed: 22203960]

21. Laan M, et al. Autoimmune regulator deficiency results in decreased expression of CCR4 and CCR7 ligands and in delayed migration of CD4+ thymocytes. J Immunol. 2009; 183:7682–7691. [PubMed: 19923453]

22. Uhlen M, et al. Proteomics. Tissue-based map of the human proteome. Science. 2015; 347:6220.

23. Kumar V, et al. The autoimmune regulator (AIRE), which is defective in autoimmune polyendocrinopathy-candidiasis-ectodermal dystrophy patients, is expressed in human epidermal and follicular keratinocytes and associates with the intermediate filament protein cytokeratin 17. Am J Pathol. 2011; 178:983–988. [PubMed: 21356351]

24. Anderson MS, et al. Projection of an immunological self shadow within the thymus by the aire protein. Science. 2002; 298:1395–1401. [PubMed: 12376594]

25. Barboro P, Ferrari N, Balbi C. Emerging roles of heterogeneous nuclear ribonucleoprotein K (hnRNP K) in cancer progression. Cancer Lett. 2014; 352:152–159. [PubMed: 25016060]

26. Pitkanen J, Vahamurto P, Krohn K, Peterson P. Subcellular localization of the autoimmune regulator protein. characterization of nuclear targeting and transcriptional activation domain. J Biol Chem. 2001; 276:19597–19602. [PubMed: 11274163]

27. Akiyoshi H, et al. Subcellular expression of autoimmune regulator is organized in a spatiotemporal manner. J Biol Chem. 2004; 279:33984–33991. [PubMed: 15150263]

28. Lallemand-Breitenbach V, de The H. PML nuclear bodies. Cold Spring Harb Perspect Biol. 2010; 2:a000661. [PubMed: 20452955]

29. Gaetani M, et al. AIRE-PHD fingers are structural hubs to maintain the integrity of chromatin-associated interactome. Nucleic Acids Res. 2012; 40:11756–11768. [PubMed: 23074189]

30. Liao J, Lowthert LA, Ghori N, Omary MB. The 70-kDa heat shock proteins associate with glandular intermediate filaments in an ATP-dependent manner. J Biol Chem. 1995; 270:915–922. [PubMed: 7529764]

31. Kumeta M, Hirai Y, Yoshimura SH, Horigome T, Takeyasu K. Antibody-based analysis reveals "filamentous vs. non-filamentous" and "cytoplasmic vs. nuclear" crosstalk of cytoskeletal proteins. Exp Cell Res. 2013; 319:3226–3237. [PubMed: 23911988]

32. Kosugi S, Hasebe M, Tomita M, Yanagawa H. Systematic identification of cell cycle-dependent yeast nucleocytoplasmic shuttling proteins by prediction of composite motifs. Proc Natl Acad Sci U S A. 2009; 106:10171–10176. [PubMed: 19520826]

33. Abramson J, Giraud M, Benoist C, Mathis D. Aire's partners in the molecular control of immunological tolerance. Cell. 2010; 140:123–135. [PubMed: 20085707]

34. Lenardo MJ, Baltimore D. NF-kappa B: a pleiotropic mediator of inducible and tissue-specific gene control. Cell. 1989; 58:227–229. [PubMed: 2665943]

35. Pasparakis M. Role of NF-kappaB in epithelial biology. Immunol Rev. 2012; 246:346–358. [PubMed: 22435565]

Methods Only References

36. McGowan KM, et al. Keratin 17 null mice exhibit age- and strain-dependent alopecia. Genes Dev. 2002; 16:1412–1422. [PubMed: 12050118]

37. Reichelt J, Haase I. Establishment of spontaneously immortalized keratinocyte lines from wild-type and mutant mice. Methods Mol Biol. 2010; 585:59–69. [PubMed: 19907996]

38. Ran FA, et al. Genome engineering using the CRISPR-Cas9 system. Nat Protoc. 2013; 8:2281–2308. [PubMed: 24157548]

39. Lessard JC, et al. Keratin 16 regulates innate immunity in response to epidermal barrier breach. Proc Natl Acad Sci U S A. 2013; 110:19537–19542. [PubMed: 24218583]

40. Adamson KA, Pearce SH, Lamb JR, Seckl JR, Howie SE. A comparative study of mRNA and protein expression of the autoimmune regulator gene (Aire) in embryonic and adult murine tissues. J Pathol. 2004; 202:180–187. [PubMed: 14743500]

41. Wan F, et al. Ribosomal protein S3: a KH domain subunit in NF-kappaB complexes that mediates selective gene regulation. Cell. 2007; 131:927–939. [PubMed: 18045535]

42. Fu K, et al. Sam68 modulates the promoter specificity of NF-κB and mediates expression of CD25 in activated T cells. Nat Commun. 2013; 4:1909.10.1038/ncomss2916 [PubMed: 23715268]
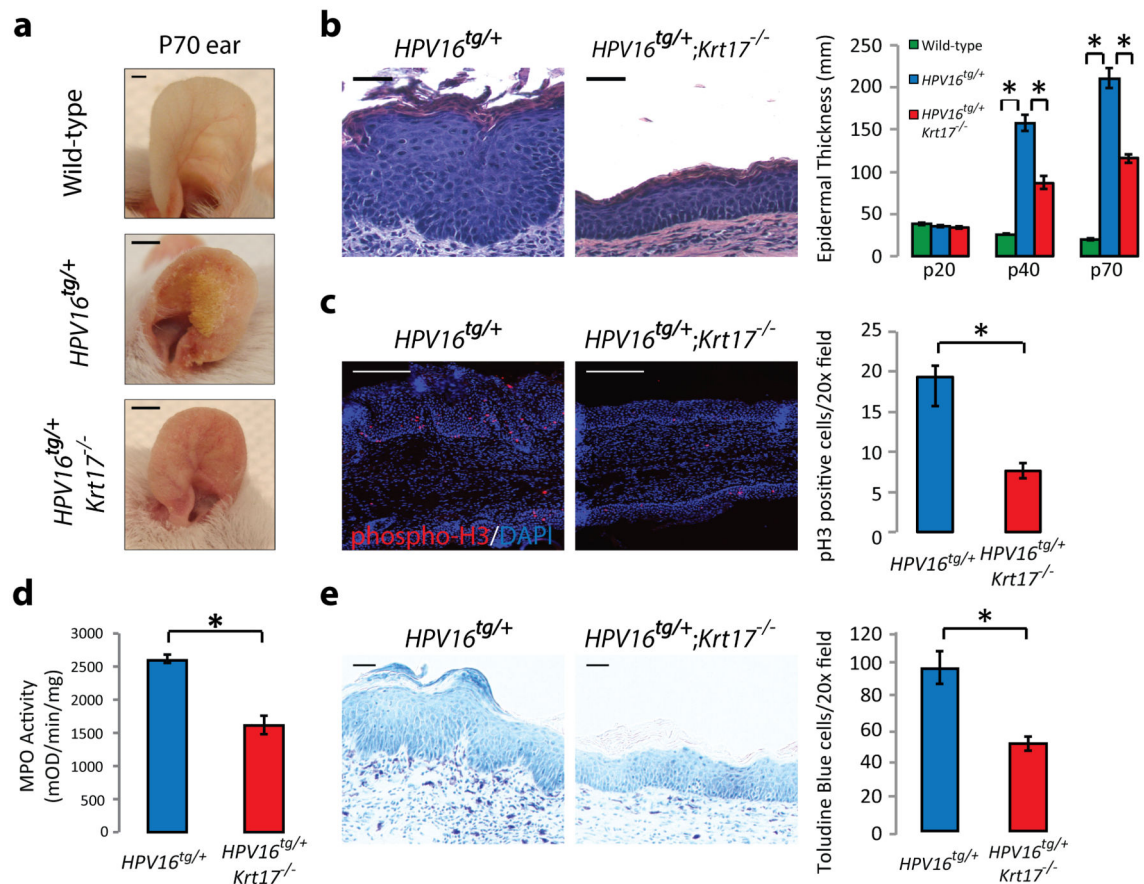
Figure 1. Loss of *Krt17* attenuates *HPV16^tg*-induced skin tumorigenesis

a) Macroscopic images of P70 ears from wild-type, *HPV16^{tg/+}*, or *HPV16^{tg/+};Krt17^{-/-}* mice. Scale bars = 1 cm. **b)** H&E staining of P70 mouse ear tissue sections and quantitation of average epidermal thickness at P20 (n = 51), P40 (n = 54), and P70 (n = 28) across genotypes. n = number of biological replicates. Scale bars = 20 μm. Error bars are s.e.m. **c)** Immunostaining and quantitation (n = 6 biological replicates) of phospho-Histone H3 (red) in P70 mouse ear tissue sections. Hoescht DNA stain (blue). Scale bars = 20 μm. Error bars are s.e.m. **d)** Myeloperoxidase (MPO) activity assay for neutrophil activation (n = 3 biological replicates, each with 4 techinical replicates). Error bars are s.e.m. **e)** Toluidine blue staining and quantitation (n = 6 biological replicates) of mast cells in P70 ear tissue sections. *p<0.05. Scale bars = 20 μm. Error bars are s.e.m.
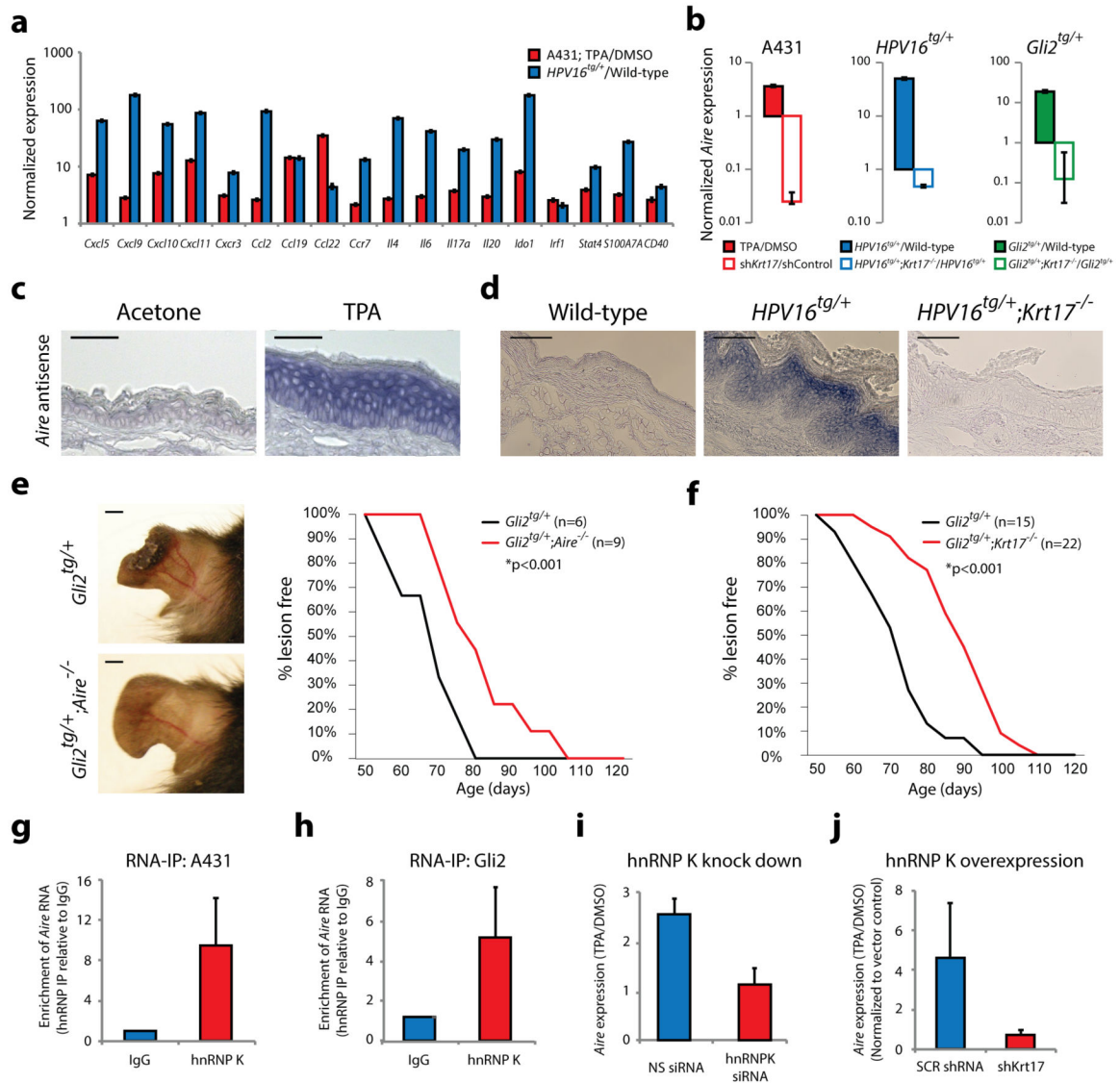
Figure 2. *Aire* expression, function, and regulation in skin tumor keratinocytes
a) Normalized expression for 18 of 19 gene transcripts common to A431 (red, n = 5 biological replicates) and *HPV16^{tg/+}* (blue, n = 6 biological replicates) paradigms. Error bars are s.e.m. **b)** Normalized expression for *Aire* (the 19th gene target) transcript levels in A431 (red), *HPV16^{tg/+}* (blue) and *Gli2^{tg/+}* (green) paradigms with (solid bars) or without (open bars) *Krt17* expression. Error bars are s.e.m. **c)** *Aire* RNA in situ hybridization (ISH) in wild-type FVB/N mouse ear tissue sections treated with acetone or TPA. Scale bars = 10 μm. **d)** *Aire* ISH in ear tissue sections from age-matched wild-type, *HPV16^{tg/+}*, and *HPV16^{tg/+};Krt17^{-/-}* mice. Scale bars = 20 μm. **e)** P80 mouse ears from *Gli2^{tg/+}* and *Gli2^{tg/+};Aire^{-/-}* littermates. Scale bars = 1 cm. Graph depicts percent *Gli2^{tg/+};Aire^{-/-}* (n = 9) mice lesion-free over time relative to *Gli2^{tg/+}* littermates (n = 6). **f)** Graph depicts percent of *Gli2^{tg/+};Krt17^{-/-}* mice (n = 22) lesion-free over time relative to *Gli2^{tg/+}* littermates (n = 15). **g-h)** Enrichment of *Aire* transcript with hnRNP K immunoprecipitation (RNA-IP) relative to IgG control in A431 keratinocytes (n = 9 biological replicates) and *Gli2^{tg/+}* keratinocytes in

primary culture (n = 9 biological replicates). Error bars are s.e.m. **i)** TPA-induced *Aire* transcript levels in A431 keratinocytes expressing non-silencing (NS) or hnRNPK-targeting siRNA oligos (n = 7 biological replicates). Error bars are s.e.m. **j)** TPA-induced *Aire* transcript levels in A431 keratinocytes overexpressing hnRNP K while stably expressing shRNA targeting *Krt17* (sh*Krt17*), relative to scrambled (SCR) sequence (n = 3 biological replicates). Error bars are s.e.m.
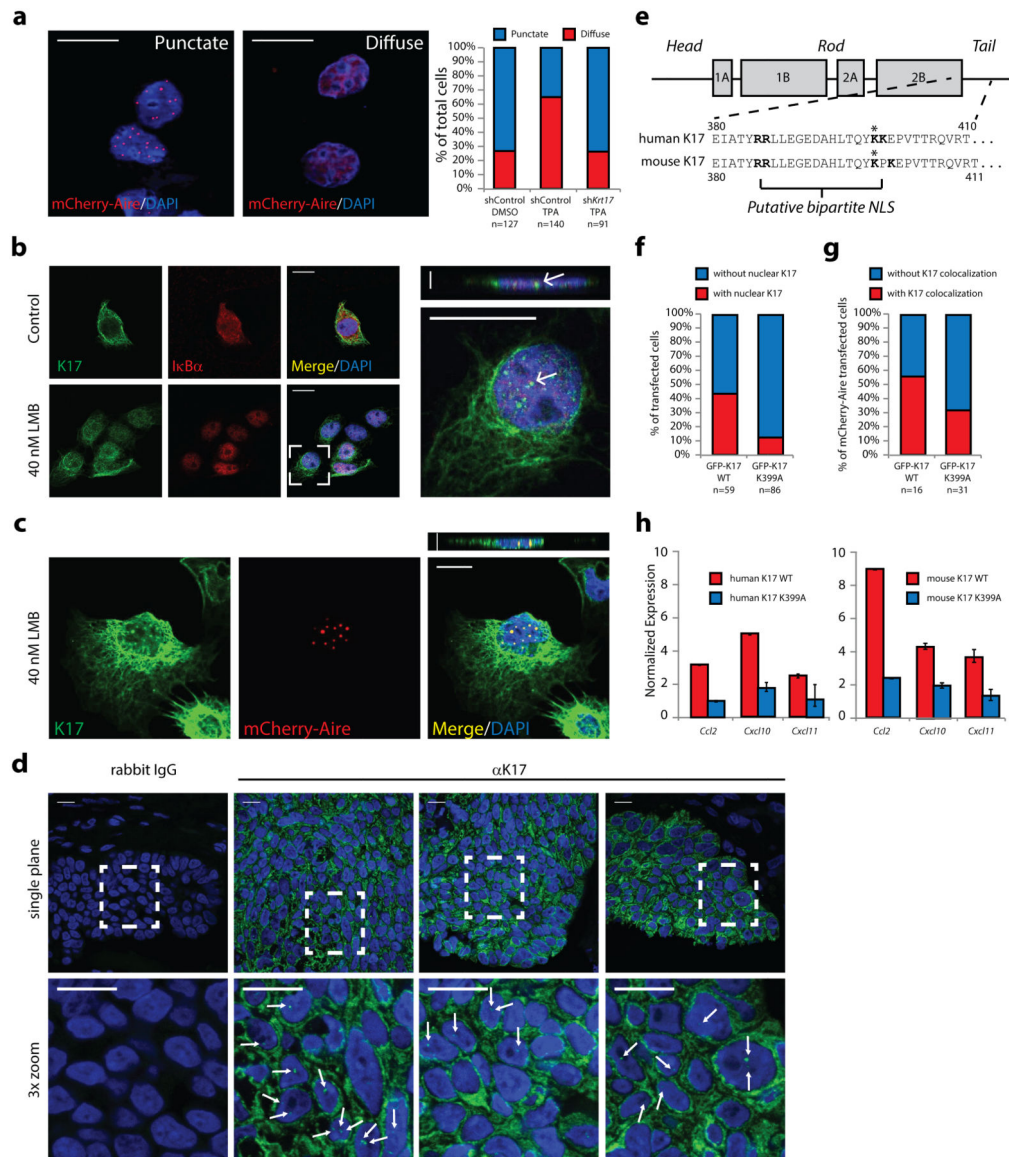
Figure 3. K17 regulates Aire subnuclear distribution and localizes to the nucleus to promote gene expression

a) Apotome-acquired images of subnuclear distribution of mCherry-Aire in A431 keratinocytes. Graph indicates percentage of cells showing punctate (blue) or diffuse (red) pattern following TPA treatment, relative to DMSO. sh*Krt17*, cells stably expressing shRNA targeting *Krt17*. n = number of cells analyzed. **b)** Single-plane confocal images of control- or leptomycin (LMB)-treated A431 keratinocytes immunostained for K17 and IκBα (positive control for LMB treatment). Inset at right highlights K17-positive nuclear punctae (arrows) and includes z-plane image. **c)** Same as in 3b, except A431 cells were transfected with mCherry-Aire prior to treatment and K17 immunostaining. Images in a, b, and c are representative from 15, 10, and 5 distinct experiments, respectively. Scale bars = 5 μM (a-c), 1 μm (z-planes). **d)** Single-plane confocal images of K17 immunostaining (or rabbit IgG control) in tissue sections of human skin basal cell carcinoma. Bottom frames, 3× digital zooms of boxed regions in top row. Arrows denote K17-positive nuclear punctae. Scale bars

= 20 μm. **e)** Schematic of keratin protein highlighting a conserved, predicted, bipartite nuclear localization sequence (NLS) (in bold letters). Asterisk denotes Lys399. **f)** Graph depicting percent of HeLa cells with nuclear punctae positive for GFP-K17, wild-type (WT) or K399A (NLS mutant), as observed by confocal microscopy. n = number of cells. **g)** Graph depicting percent of A431 cells where mCherry-Aire punctae colocalize with GFP-K17 WT or GFP-K17 K399A. n = number of mCherry-Aire positive cells counted. **h)** Normalized expression of TPA-induced target gene transcript levels in A431 *Krt17* null keratinocytes transfected with GFP-K17 WT or GFP-K17 K399A, either human (left) or mouse (right) species. n = three biological replicates. Error bars are s.e.m.
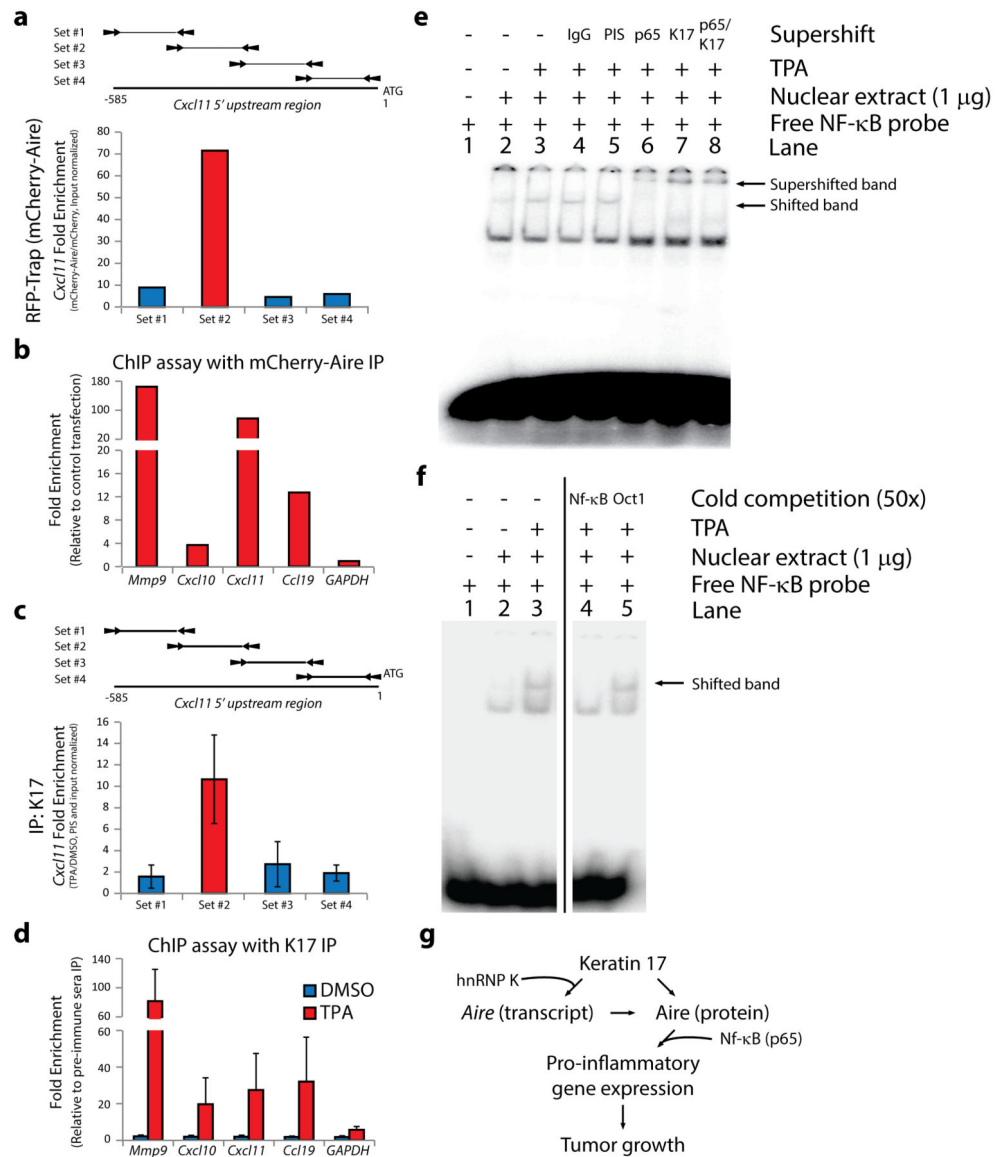
Figure 4. K17 and Aire associate with target gene promoter regions
a) Representative ChIP assay from A431 keratinocytes depicting enrichment of a specific 5′upstream sequence of *CXCL11* transcript following mCherry-Aire immunoprecipitation, relative to unfused mCherry. Schematic of the 5′upstream region for *Cxcl11* with locations of qRT-PCR primer sets is provided. **b)** Summary of ChIP assays depicting enrichment of single DNA segments within the 5′upstream sequence of select genes with mCherry-Aire IP relative to unfused mCherry. **c)** Summary of ChIP assays using K17 IP, relative to pre-immune sera (PIS) control, depicting TPA-induced enrichment of the same 5′upstream sequence of the *CXCL11* transcript as in Fig. 4a. n = seven biological replicates. Error bars are s.e.m. **d)** Summary of ChIP assays using K17 IP, relative to pre-immune sera control, depicting the TPA-induced enrichment of single DNA segments within the 5′upstream sequence of select genes. n=7 biological replicates. Error bars are s.e.m. **e)** EMSA analysis of radiolabeled NF-κB consensus oligonucleotides using nuclear extracts from A431

keratinocytes treated with TPA, relative to DMSO control. Supershift analysis was conducted with antibodies against p65 (lane 6) and K17 (lane 7), relative to anti-IgG (lane 4) and PIS (lane 5) controls. Image represents 1 of 5 biological replicates. **f)** Cold competition EMSA analysis using nuclear extracts and radiolabeled oligonucleotide as in e) with inclusion of 50-fold excess non-labeled oligonucleotide (lanes 4-5). Image represents 1 of 3 biological replicates. **g)** K17 regulates Aire at both the transcript and protein levels to promote inflammatory gene expression and skin tumorigenesis.